Actuated Passive Dynamic Walker Control: Stable Walking with Varying Hip Mass and Ramp Angle

Rebecca Agustin[1] and Shang-Yun (Maggie) Wu[2]

Abstract— Passive dynamic walkers and their ability to intuitively mimic humans walking down a slope with minimal energy have been extensively studied throughout the past decade. The most common version is the two-legged robot known as the compass gait and its passive physical system dynamics. In this paper, we explore the design of more robust passive dynamic walkers–specifically, a modified compass gait walker that can adjust to perturbations in hip mass and ramp angle through control of an actuated hip joint. The feedback controller described in this paper takes into consideration the relative swing and stance angle to determine necessary torque in order to restore the system back to passive walking. Our results suggest that while varying hip mass induces minimal effects to the system, varying the ramp angle presents interesting challenges towards designing a robust controller with carefully chosen parameters.

I. INTRODUCTION

In the past, passive dynamic walkers have been extensively studied with insightful breakthroughs. This is particularly true with the two-legged passive dynamic walker known as the compass gait. This paper examines the behavior of a compass gait walker in an environment with varying hip mass and ramp angle. Using a single actuator at the hip, one can control the between-leg angle of the compass gait in order to facilitate continuous passive dynamic walking under a wider range of conditions. In response to an altered hip mass and ramp angle, the actuator provides minimal but sufficient torque to change the between-leg angle such that the system continues to walk without interruption.

This perspective of the compass gait walker is interesting due to its possible practical applications in the field of robotics. From a real-world perspective, the slight perturbations in ramp angle that are randomly applied to our system can be viewed as noises in an overall downhill environment while the changes in hip mass can simulate a situation wherein a robot based on the compass gait walker is loaded and unloaded with objects as it traverses the aforementioned downhill slope. More concretely, a robot based off of this version of the compass gait walker would be able to carry packages of varying weights throughout its trip on a non-uniformly leveled surface as simulated by the varying ramp angle [1]. The ability to complete such a task would ultimately bring insights into the design of other

adaptive robot behaviors. Additionally, an understanding of this system could potentially apply to various types of passive dynamics walkers [2].

The following sections are broken down as such: a review of previous research and studies related to maintaining compass gait stability in non-standard conditions; an in-depth explanation of the compass gait control approach in this study; a summary of its corresponding results; and finally a discussion regarding the implications of these results for further research involving passive dynamic walkers.

II. RELATED WORK

A. Speed, Efficiency and Stability

There has been a great deal of work done in the past to understand the dynamics of the compass gait walker. At a high level, these passive dynamic walkers utilize gravity to provide a periodic motion resembling a human walking down a ramp. For these underactuated systems, efficiency is highly correlated to energy loss, which can be mitigated via small actuation. Additions to the compass gait system, such as a toe-off force, have been studied to provide minimal but effective energy to the system in order to maximize efficiency [3]. Overall, the focus of passive dynamic walking is primarily towards energy efficiency rather than simplicity of control strategies. To achieve this, compass gait walkers are designed to mimic the dynamics of human walking without exerting energy. The stability of the passive dynamic walker can be analyzed via its limit cycle.

B. Adding Upper Body Mass

Most studies done on the passive dynamic walker focus on robot leg mass with little emphasis on hip mass. In 2007, Wisse et al proposed adding a significant upper body mass and achieving balance and stability with a two-legged compass gait [4]. This particular compass gait is setup in a way similar to the standard cart-pole system; the existence of an upper body, which further increases the system's resemblance to human walking dynamics, means that balancing this structure becomes a major component of the compass gait control approach. With fine-tuning of the hip spring and slope angle as well as a series of carefully selected parameters, the robot from this study is able to achieve stable speed and step size that fit human values. However, there are limits to the conditions where stability is possible; in the case of highly-slanted angles, the stable speed of the compass gait is too fast to reliably maintain foot contact with the ramp.

*The authors contributed equally to this project

[1]Rebecca Agustin is with the Department of Electrical Engineering and Computer Science, Massachusetts Institute of Technology, Cambridge, MA 02139, USA `agustinr@mit.edu`

[2]Shang-Yun (Maggie) Wu is with the Department of Electrical Engineering and Computer Science, Massachusetts Institute of Technology, Cambridge, MA 02139, USA `maggiewu@mit.edu`

C. Control for Various Speed in PDW

In another study from 2012, Liu et al proposed a controller design based on Lyapunov stability theory and feedback linearization techniques [5]. Using the Lyapunov function, the controller adjusts smoothly between different gait speeds. At the same time, it expands the range of achievable yet regulated speeds. The simulation results presented in the paper suggest great success in both efficiency and robustness.

III. APPROACH

The three major components in this study involve analyzing the compass gait's dynamics, implementing a compass gait simulator using PyDrake, and applying a proportional feedback controller to regulate the compass gait in the face of small perturbations. Each of the three components will be explained in detail below, illustrating the benefits and drawbacks of our approaches.

A. Analysis of Compass Gait

The compass gait walker modelled in our study is shown in Figure 1. In this case, the swing and stance angles are presented with respect to the world frame as opposed to the ramp frame of reference and are measured in opposite directions. The ramp angle is denoted as α with units of radians. The hip and leg masses are denoted as m_h and m_l, respectively, where m_l is set to 5kg for all conditions.
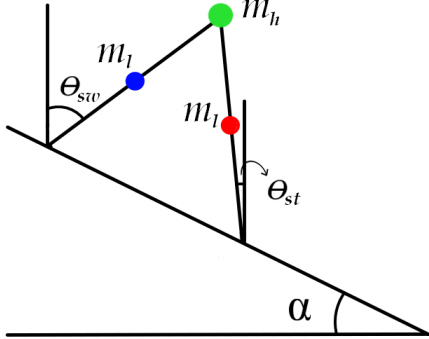

Fig. 1.   Standard Compass Gait Structure

B. Simulator

The simulator for the compass gait walker in our study includes input parameters for a varying ramp angle and an adjustable hip mass. The original compass gait simulator provided in the PyDrake binding does not support dynamic changes to the compass gait parameters since it calls directly from the c++ code in the standard Drake library. Therefore, in order to account for the changing parameters in our study, an alternative Python-based implementation is written for the same class.

The updated simulator creates a simple compass gait model with parameters of one's choosing. Since the goal of our study is to analyze the effects of changing hip mass and changing ramp angle, these are the only variables that can be inherently altered when creating a new compass gait model. However, simple modifications to this compass gait implementation may be made if necessary in order to tune parameters inherent to the simulator.

Functionalities of the compass gait model include the ability to set the toe position and stance leg, calculate collision dynamics of the system, and update the state of the model at every time step. First, the toe position is determined by the swing and stance angle of the compass gait. Meanwhile, the current stance leg alternates as the compass gait model walks down the ramp. Next, calculating the dynamics of the system allows the model to check for collisions between the legs and the ramp while the compass gait is in motion. However, in the case where the swing leg collides with the ramp while passing the stance leg, the collision is ignored in order to account for the clearance of the swing leg. Finally, derivative updates are calculated in order to dynamically change the state of the model. This update is written with respect to the manipulator equation:

$$M(q)\ddot{q} + C(q,\dot{q})\dot{q} = \tau_g(q) + Bu \tag{1}$$

where the matrices are defined as follows:

$$M = \begin{bmatrix} (m_h + m)l^2 + ma^2 & -mlb\cos(\theta_{st} - \theta_{sw}) \\ -mlb\cos(\theta_{st} - \theta_{sw}) & mb^2 \end{bmatrix}$$

$$C = \begin{bmatrix} 0 & -mlb\sin(\theta_{st} - \theta_{sw})\dot{\theta}_{sw} \\ mlb\sin(\theta_{st} - \theta_{sw})\dot{\theta}_{st} & 0 \end{bmatrix}$$

$$\tau_g = \begin{bmatrix} (m_h l + ma + ml)g\sin(\theta_{st}) \\ -mbg\sin(\theta_{sw}) \end{bmatrix}$$

$$B = \begin{bmatrix} 1 \\ -1 \end{bmatrix}$$

For the completely passive compass gait, the control input u is essentially 0, allowing the system to operate solely with respect to its own dynamics. In other words, $\ddot{q}$ is determined by the inverse of the mass matrix and the bias term. However, with an actuator at the hip providing torque, the control vector Bu has a greater influence when determining $\ddot{q}$:

$$\ddot{q} = -M^{-1}[C - \tau_g - Bu] \tag{2}$$

It is important to note that the signs of the B matrix components depend on the definition of the stance and swing angle with respect to the world frame. Given the definition provided in Figure 1, the two components of B will be of opposite signs.

The model is based on a Floating Base output since a minimal state does not allow for dynamic changes of the compass gait parameters. At the same time, the energy of the system is calculated each time step as part of the proportional controller, which is further explored in the following section.

The simulator is setup to run for 10 seconds for various perturbations as modelled by different initial conditions. Corresponding stabilization times and parameters are shown in Table 1. The logger for the simulator publishes the robot's

state every 0.033 seconds. Corresponding $\theta_{st}, \theta_{sw}, \dot{\theta}_{st}, \dot{\theta}_{sw}$, and u are plotted for better visualization.

C. Feedback Proportional Controller

The feedback controller must fulfill three major conditions in order to maintain a relatively stable system.

1) Minimal Collision: Although the collision of the swing leg as it moves forward and passes the stance leg is ignored, additional collisions remain valid. Therefore, it is essential to ensure that there exists enough clearance between the ramp and the swing leg after the swing leg passes the stance leg so that the swing leg does not cause the compass gait to trip forward. A simple condition can be imposed where the swing leg must pass the stance leg before the falling of the stance leg causes itself to become perpendicular to the ramp, as illustrated in Figure 2. If this condition is met, the swing leg is guaranteed not to collide with the ramp at any other time than the moment of passing the stance leg, which is effectively ignored, and the actual step of foot placement.
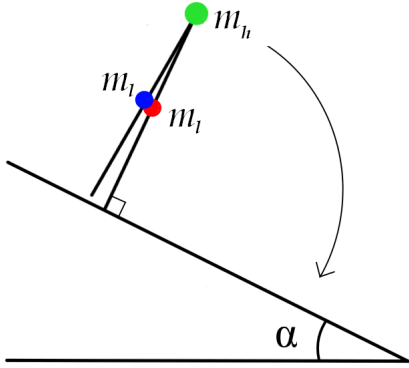

Fig. 2.   Falling Forward Compass Gait

Given the setup of the system shown in Figure 1, the inequality associated with this condition is formulated below:

$$\theta_{sw}^{ramp} = \theta_{sw} + \left(\frac{\pi}{2} - \alpha\right)$$

$$\theta_{st}^{ramp} = \theta_{st} + \left(\frac{\pi}{2} - \alpha\right)$$

Let t_{perp} be the time when the swing leg passes the stance leg. The corresponding swing leg angle in ramp frame of reference would then be:

$$\theta_{sw}^{ramp}(t_{perp}) \sim \theta_{sw}^{ramp}(0) + \dot{\theta}_{sw}(0)t_{perp}$$

where t_{perp} is determined by the stance angle

$$\theta_{st}^{ramp}(t_{perp}) = \frac{\pi}{2} \sim \theta_{st}^{ramp}(0) + \dot{\theta}_{st}(0)t_{perp}$$

$$t_{perp} = \frac{\frac{\pi}{2} - \theta_{st}^{ramp}(0)}{\dot{\theta}_{st}(0)} \tag{3}$$

Due to the small overall swing leg angle and the short duration of the passing movement, the effect of gravity is ignored for the t_{perp} calculation. Given t_{perp}, the controller can be designed accordingly:

$$\theta_{sw}^{ramp} \sim \theta_{sw}^{ramp}(0) + \dot{\theta}_{sw}^{des}(0)t_{perp} < \frac{\pi}{2} - \epsilon$$

$$\dot{\theta}_{sw}^{des}(0) < \frac{\frac{\pi}{2} - \epsilon - \theta_{sw}^{ramp}(0)}{t_{perp}}$$

$$\dot{\theta}_{sw}^{des} = \dot{\theta}_{sw}(0) + \ddot{\theta}_{sw}t = \dot{\theta}_{sw}(0) + ut$$

$$u = \frac{\dot{\theta}_{sw}^{des} - \dot{\theta}_{sw}(0)}{t} \tag{4}$$

Equation (4) assumes a small ϵ and t value to ensure near instantaneous change given a reasonable control input. In other words, the choice of t is the effective gain on the control input u, which is further fine-tuned for smooth simulation. Values of $\epsilon = 0.05$ and $t \in [1, 20]$ are found to work sufficiently well for the simulations in our study.

2) Sufficient Momentum: So far, the controller addresses one failure condition where the falling of the compass gait with respect to its swing rate is fast enough to cause the compass gait to trip forward. However, it does not take into consideration the condition where the system lacks the necessary momentum for continuous motion. Even though the swing leg is given enough torque to move forward at a speed that allows it to clear the ramp without unplanned collisions, the entire compass gait could easily fall backwards due to a lack of momentum under certain settings, as shown in Figure 3.
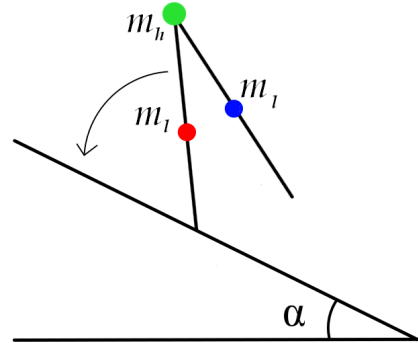

Fig. 3.   Falling Backward Compass Gait

Our final controller addresses this by initially supplying a torque to drive the compass gait until it can walk stably. This torque is proportional to the difference between the swing and stance leg angles so that sufficient but not excess momentum is given to drive the swing leg forward without causing the robot to trip over its own swing leg. Thus, the final controller is:

$$u = k_p * (\theta_{sw} - \theta_{st}) \tag{5}$$

The constant k_p changes in magnitude depending on if θ_{sw} is greater or smaller than θ_{st} in order to account for the asymmetric force on the swing leg when it is in front, rather than behind, the stance leg. Depending on the stage of the swing motion, the impact of gravitational forces on the swing leg will change in magnitude. For similar reasons, the ratio between the k_p values in each scenario varies according to the ramp angle as the effect of gravity on the compass gait's forward motion changes.

Experiments suggest that $k_p \in [1, 20]$ works reasonably well for a range of ramp angles $\alpha \in [0.01, 0.1]$. Most falling conditions are caused at the instant of perturbation. Therefore, the extra torque from the controller is only supplied at the beginning of the perturbation until stability is achieved. The model is found to stabilize in less than 3 seconds for various conditions given carefully chosen gain values. However, to account for any additional falling conditions happening further down the ramp, kinetic and potential energy are constantly calculated with small amounts of torque applied when either falls out of their respective periodic stable cycles.

3) Torque Limit: The compass gait hip actuator has a maximum and minimum torque that it can possibly supply at any time. To reflect this, the control input is limited so that no more than $|u| = 10$ can be supplied. As a result, there remains certain initial conditions where the torque cannot sufficiently drive the compass gait back to a stable cycle before it trips forward or loses sufficient driving momentum as stated in the conditions described previously.

IV. DISCUSSIONS

A. Varying Mass

In the standard setup, the hip has a mass of 10kg while the legs are each 5kg. Keeping the ramp constant, the variations in mass yield little to no difference in the stable walking condition. This makes sense since the stable walking condition is achieved via balanced walking and changes in the hip mass do not alter the compass gait's overall balance.

However, in the case of an extremely small hip mass, for instance 0.1kg, the "stable" walking condition is rather unsteady with an unusual periodic motion. This makes intuitive sense since, as the compass gait switches its stance leg, the majority of the weight shifts onto the new stance leg. Compared to a compass gait with a larger mass at the hip, the position of the center of mass for a compass gait with a small hip mass moves more significantly during the walking process, causing the system to be comparatively unstable. This may be further illustrated by the small region of attraction found when varying ramp angle with a small hip mass.

The results comparing the effect of varying hip mass (values = 0.1, 10, and 100kg) are shown in Figures 4-6. The stance and swing leg angles are more periodic and consistent for hip masses of 10kg and 100kg compared to those in the 0.1kg hip mass, as explained above.
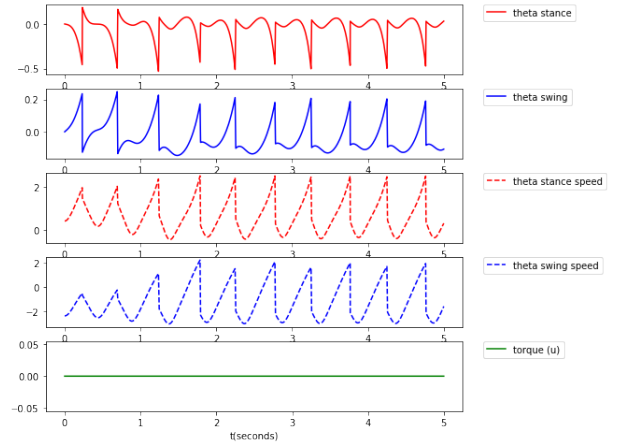

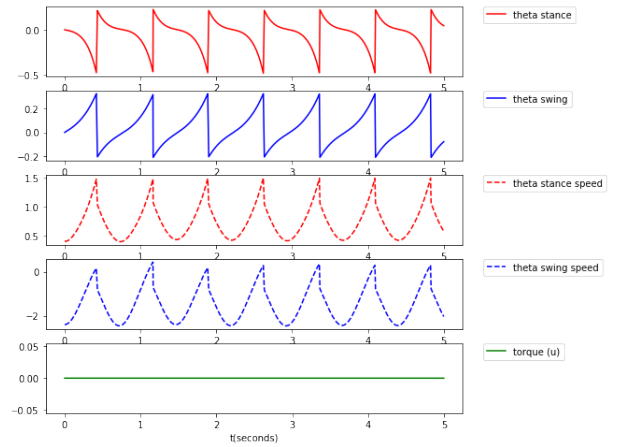Fig. 4.   10s Walking Condition for Hip Mass = 0.1kg

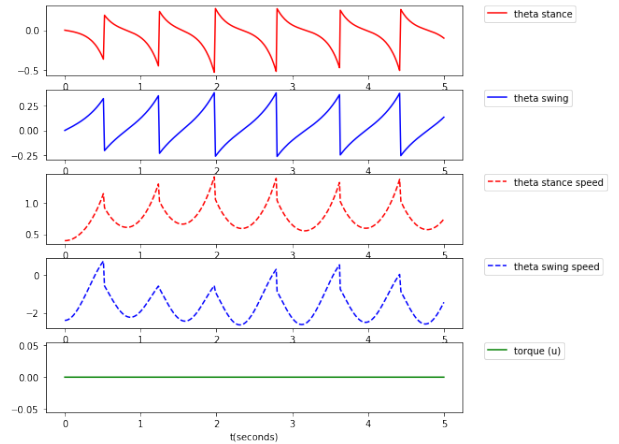
Fig. 5.   10s Walking Condition for Hip Mass = 10kg

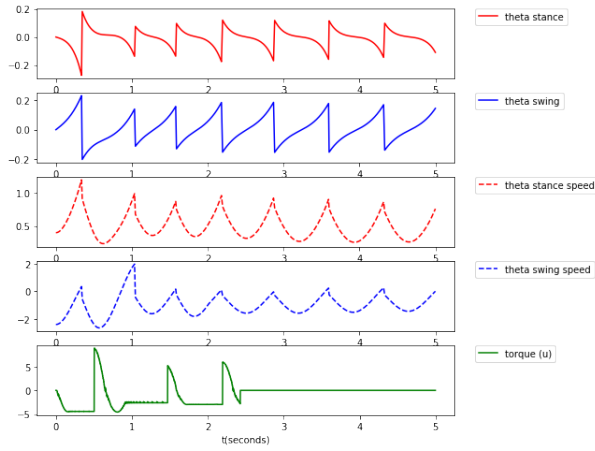Fig. 6.   10s Walking Condition for Hip Mass = 100kg
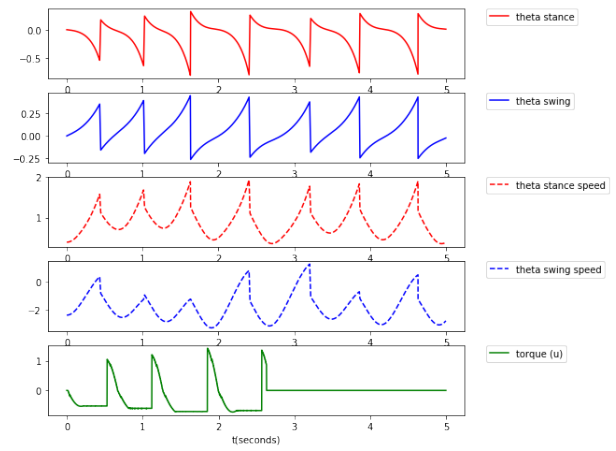
Fig. 7.   10s Walking Condition for Slope = 0.01

Fig. 8.   10s Walking Condition for Slope = 0.1

B. Varying Ramp

The effect of varying ramp angle is significantly more critical to the stable walking condition compared to that of varying hip mass. In order to prevent the compass gait from falling, a feedback controller is used to address conditions with different ramp angles.

In order to achieve stable walking, an increase in ramp angle necessitates a decrease in torque input from the controller. Increasing ramp angle is equivalent to creating a condition where gravity has a stronger effect on the swing leg of the compass gait. Therefore, less external torque, even at times a negative torque, is required to successfully drive the system forward.

Various simulation results suggest that stability is achieved within 3 seconds of effective controlling. This suggests that the system can restore itself to a stable walking state within a small amount of time with respect to some perturbation. This restoration time is proportional to the amount of perturbation - more perturbation generally requires more time to stabilize. However, when the perturbation is too large, the simulator is unable to run to completion, suggesting potential numerical instability within the simulator given large changes.

The results comparing the effect of varying ramp angle (values = 0.01 and 0.1 radians) are shown in Figures 7-8. The tracking of the control input in these figures supports the argument regarding gravitational acceleration - a steeper ramp requires less torque input.

C. Limit Cycles

Limit cycle plots are shown in Figures 9-10 for varying hip mass and varying ramp angle conditions. To avoid repetition of the same limit cycle, only the last 10% of the data for each condition is plotted. Since the varying hip mass condition requires no torque input to walk stably, there is no measure of convergence rate. On the other hand, the convergence rate to stable limit cycle for varying ramp angle condition is shown in Table 1. Additionally, since the limit cycles shown are based on the swing leg, the jump from right to left is visible as the swing legs change.

As discussed in the previous section regarding the varying mass condition, the limit cycle is consistent for hip mass greater than or equal to $5kg$. Not only can we intuitively see such stability in our simulation, but also in the limit cycle plots which support the controller's robustness with respect to a varying mass condition. However, when the hip mass becomes too small, the stable limit cycle takes a different shape as the hip mass contributes less to the center of mass. In this case, the leg mass dominates the limit cycle.

On the other hand, the limit cycles for varying ramp angle mostly follow the same general pattern. This supports our intuitive understanding about the compass gait–the steeper the ramp, the wider the stable walking gait. In other words, as the ramp angle increases, the sizes of the limit cycles also increase. Although controller gains must be carefully chosen to drive the system to stability, upon reaching the limit cycle, no additional torque is required. In the case of very steep ramps ($\alpha \geq 0.1$), the limit cycle pattern is no longer present. This is due to the initial setting of the compass gait being upright with respect to the world frame of reference. That is to say, negative torque, as illustrated in Table 1, is required to drive the system forward at the very beginning. However, since our proportional feedback controller gains remain the same throughout, the negativity of the gain will cause the limit cycle to be drastically different. It can also be theorized that given this particular ramp angle and initial condition, a stable walking condition is not necessarily reachable via our proportional feedback controller.

D. Poincare Maps

To understand the convergence behaviors of the limit cycles, which are effectively ignored in Figures 9-10 for clarity, the Poincare maps are shown in Figures 11-16.

The results for stable, no-torque conditions are shown in Figures 11 and 15 for varying hip mass and varying ramp angle. As evident in both figures, stable walking convergences towards a relatively small range of values, but not one specific fixed point. In comparison to monotonic convergence of the standard van der pol oscillator, our compass gait has an oscillatory convergence.
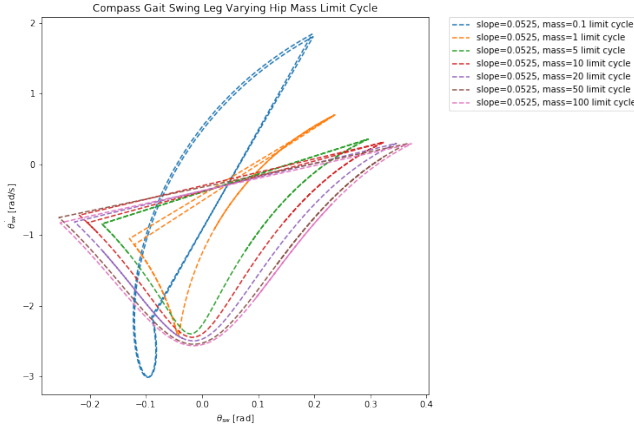
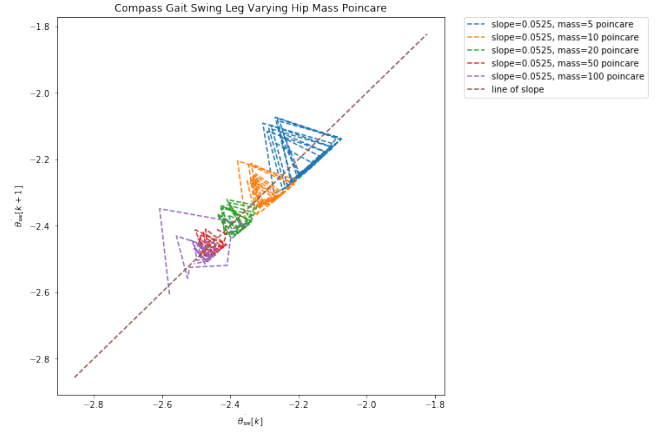Fig. 9.   Swing Leg Limit Cycles for Varying Mass

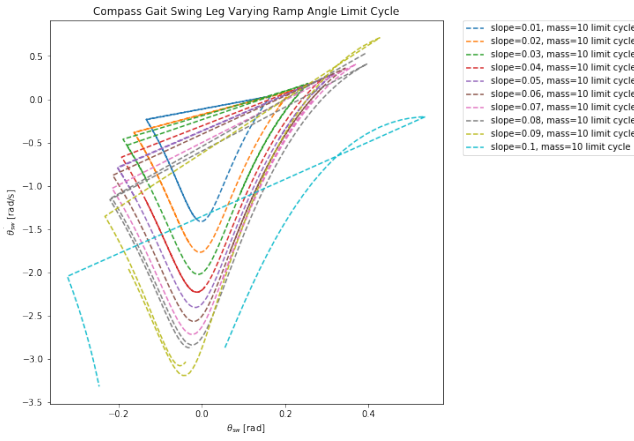Fig. 11.   Swing Leg Poincare for Masses > 1kg

Fig. 10.   Swing Leg Limit Cycles for Varying Ramp Angle
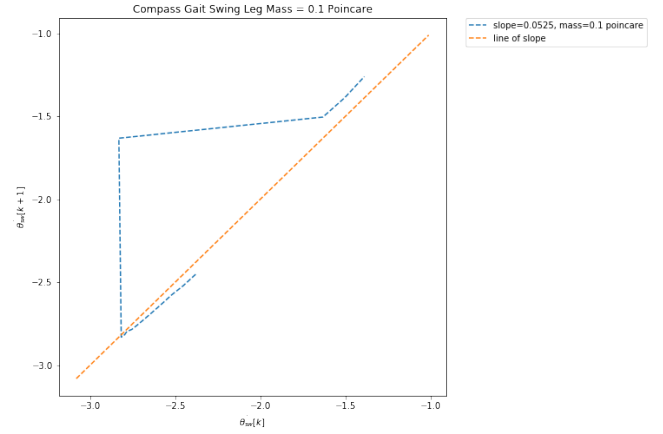

Fig. 12.   Swing Leg Poincare for Mass = 0.1kg

Similar behaviors can be seen in Figures 13 and 14 for hip mass = 1kg and low ramp angle conditions. While the oscillations have larger amplitudes and thus take longer for the systems to stabilize, the Poincare maps still illustrate stable limit cycles.

Alternatively, in Figure 12 for hip mass = 0.1kg, almost no stability can be seen. In the case of small hip mass, the walking, despite periodic, is no longer human-like. At the same time, given the constant swing of center of mass as discussed above, the point of reference for Poincare analysis may also need to be adjusted for any effective understanding of its limit cycle.

For high ramp angle conditions, our simulation shows a periodic behavior that has period of every few kicks. In other words, given the choice of our feedback controller, the compass gait walker gives a strong kick, trembles for the next 2-3 gaits and repeats. Therefore, the system would yield two stable limit cycles as opposed to one. There would be one stable limit cycle corresponding to the strong kick and another corresponding to the trembles, where the system oscillates between the two. Thus, the Poincare analysis does not stabilize to one stable fixed point due to the constant switch between these two walking conditions.

V. CONCLUSION

In our study, an actuated compass gait is studied with varying hip mass and ramp angle conditions. The Python implementation of the compass gait is written to allow for adjustments of the compass gait parameters using the manipulator equation provided in equation (1) and a torque input when necessary as formulated in equation (2). Finally, the leg angles, leg angle velocities, torque input and limit cycle analysis plots are provided for better visualization and understanding of the system.

In order to effectively control the passive walker during perturbation, the three necessary conditions (minimal collision, sufficient momentum and torque limit) for our simulator are explicitly discussed in this paper. These conditions are necessary and sufficient to guarantee restoration of a passive walker under reasonable perturbations.

Our study results suggest that varying hip mas has minimal effects on compass gait stability. Since the balance of the passive walker ensures minimal movement of the center of mass, its stability should be independent of the hip mass. Thus, only in the case of a particularly small hip mass, as shown in Figure 3, would we see greater shifts of the center of mass due to a greater emphasis on the swing leg mass.
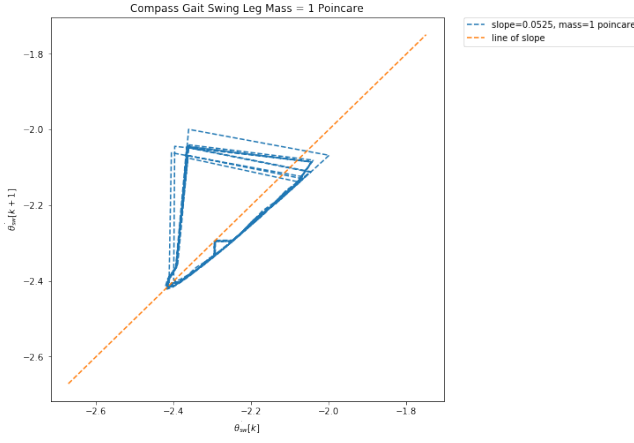
Fig. 13.   Swing Leg Poincare for Mass = 1kg
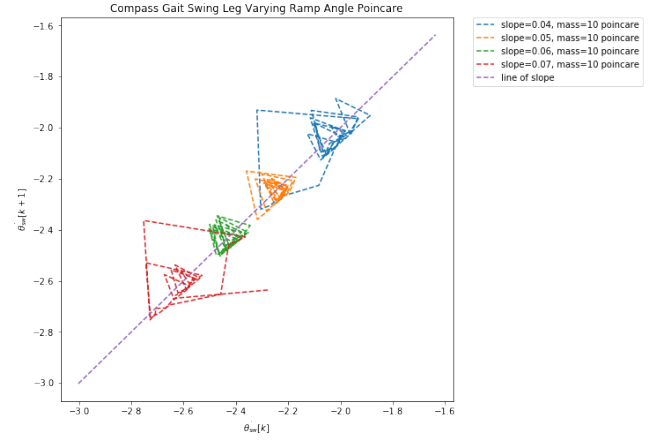

Fig. 15.   Swing Leg Poincare for Torqueless Ramp Angles
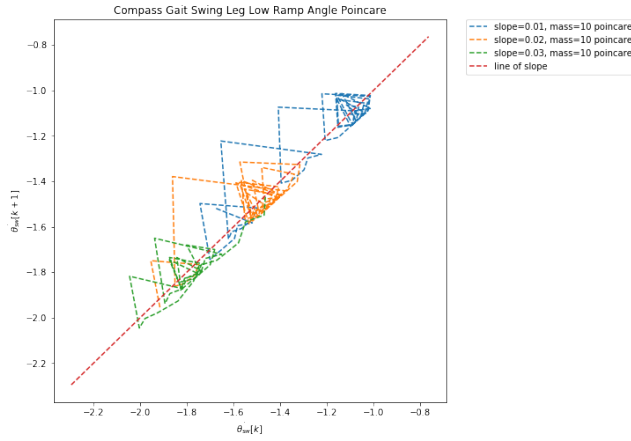

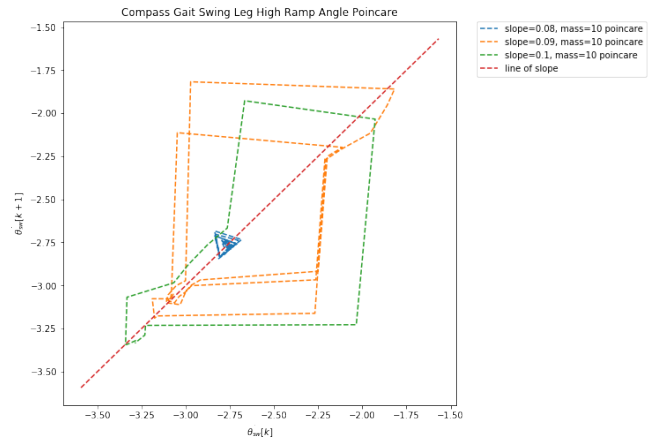Fig. 14.   Swing Leg Poincare for Low Ramp Angles

Fig. 16.   Swing Leg Poincare for High Ramp Angles

On the other hand, varying ramp angle completely changes the dynamics of the system. As a result, control input becomes necessary to restore the system to stability. In particular, a greater amount of torque is necessary to drive a passive walker on a flat ramp compared to one on a steep ramp. This is due to a difference in the effect of gravity on the forward movement of the compass gait; the steeper the ramp angle, the more gravity contributes to the forward movement and the less torque the actuator needs to provide.

The proportional feedback controller is experimentally found to be effective in regulating the system back to stability. Since the controller places emphasis on the difference in swing and stance leg angles, it sufficiently drives the compass gait forward without using excess torque and causing the robot to trip forward. This is particularly successful as only 3 seconds are required to restore the system back to stable passive walking for most standard perturbations.

While this simple controller achieves great success in driving the compass gait, additional modifications can be made to more efficiently determine the necessary torque. In the case of our study, gain values are chosen nearly arbitrarily with a general downward trend for steeper ramp angles. A more in-depth study of the basin of attraction of the system

would help determine the range of gains that would drive the system forward given specific conditions.

At the same time, energy calculation is done to minimally regulate the system, but the majority of the control effort comes from feedback with respect to the leg angles. Even though this approach is proven effective, additional study on the energy shaping of the compass gait would bring further insights for a more efficient compass gait controller. Analysis via bifurcation graph would also allow us to understand the stability of the system better.

Since this study focuses greatly on a practical implementation, many theoretical concepts are adapted from standard compass gait analyses and hypothesized to work. Further study can be done to analyze this system so that a more robust controller may be designed to reflect the dynamics of the system. With the support of analytical understanding, such a study would be more complete and translatable to other systems with similar dynamics.

APPENDIX

Implementation code can be reviewed at
https://github.com/maggiewu19/compass-gait-simulator

Mass	Angle	Gain	Time
10	0.01	15:15	2.39
10	0.02	15:15	2.43
10	0.03	4:5	0.5
10	0.04	0:0	0.00
10	0.05	0:0	0.00
10	0.06	0:0	0.00
10	0.07	0:0	0.00
10	0.08	15:8	2.36
10	0.09	2:1	2.67
10	0.1	4:-1	–

TABLE I

VARYING RAMP ANGLE STABLE GAIN VALUES

REFERENCES

[1] K. Byl and R. Tedrake, "Approximate optimal control of the compass gait on rough terrain," presented at the Int. Conf. on Rob. and Auto., 2008.

[2] K. K. Safak, "Dynamics, stability, and actuation methods for powered compass gait walkers," vol. 22, p. 16111624, Nov. 2014.

[3] A. C. M. Garcia and A. Ruina, "Efficiency, speed, and scaling of two-dimensional passive-dynamic walking," vol. 15, pp. 75–99, July 2000.

[4] D. G. E. H. M. Wisse and A. L. Schwab, "Adding an upper body to passive dynamic walking robots by means of a bisecting hip mechanism," vol. 23, pp. 112–123, Feb. 2007.

[5] L. Liu and Y. Tian, "Switch control between different speeds for a passive dynamic walker," vol. 9, Sept. 2012.